Electronic Supplementary Information

How the External Solvent in Biocompatible Reverse Micelles can Improve the

Alkaline Phosphatase Behavior

Nahir Dib[a,b]*, Valeria R. Girardi[a], Juana J. Silber[a,b], N. Mariano Correa[a,b], R. Dario

Falcone[a,b]*

[a] Departamento de Química, Universidad Nacional de Rio Cuarto, Agencia Postal 3, C.P.

X5804BYA, Ruta Nacional 36, km 601, Rio Cuarto, Córdoba, Argentina.

[b] Instituto de Desarrollo Agroindustrial y de la Salud (IDAS), Universidad Nacional de Río

Cuarto, Agencia Postal 3, C.P. X5804BYA, Ruta Nacional 36, km 601, Río Cuarto, Córdoba,

Argentina.

* Corresponding-Authors: Dr. R. D. Falcone. E-mail: rfalcone@exa.unrc.edu.ar

Dr. N. Dib. E-mail: ndib@exa.unrc.edu.ar

Experimental Section

1.1 Materials

Methyl laurate (≥98% purity), isopropyl myristate (≥98% purity), benzene (HPLC quality), n-heptane (HPLC quality), sodium 1-naphthyl phosphate (>98% purity), and alkaline phosphatase (AP) from bovine intestinal mucosa (lyophilized powder 160 kDa) were purchased from Sigma-Aldrich and used as received. The surfactant AOT, from Sigma (>99% purity), was dried at reduced pressure before use. Sodium carbonate and sodium hydrogen carbonate (>99% purity, Fluka), were used as supplied. Milli-Q (Millipore) equipment was used to obtain ultrapure water. The absence of acidic impurities was carefully checked by using 1-methyl-8-oxyquinolinium betaine as an indicator because those impurities can significantly affect the pH of the dispersed aqueous phase.[1]

The pH of the aqueous solution has been maintained at pH = 10 by using a 0.01 M sodium carbonate/sodium hydrogen carbonate (Na_2CO_3-$NaHCO_3$) buffer solution.

1.2 Methods

1.2.1 Preparation of RMs solutions

Individual solutions of RMs were prepared from AOT/nonpolar solvent stock solutions, incorporating the polar phase with calibrated microsyringes. As the polar phase, an aqueous solution composed of sodium carbonate/sodium hydrogen carbonate buffer (Na_2CO_3-$NaHCO_3$) at 0.01 M (pH = 10), was used. The content of the polar phase in the micellar solution was expressed as $W_0 = [H_2O]/[AOT]$. All the studies in the RMs were performed at $W_0 = 10$.

*1.2.2 Enzymatic Reaction in water and AOT RMs*

In a thermostated cell that contained the AP in water (0.01 M buffer solution at pH = 10), the enzymatic reaction was initiated by the addition of different µL of the stock solution of 1-naphthyl phosphate to have 3 mL of solution with the desired [1-naphthyl phosphate] and [AP] concentrations in the buffer solution. The [1-naphthyl phosphate] was varied from $5x10^{-5}$ to $5x10^{-4}$ M, and [AP] was equal to $1x10^{-7}$ M in all the experiments.

In a typical kinetic experiment in RMs, an appropriate amount of AOT/nonpolar solvent stock solution (0.2 M) was transferred into UV-vis quartz cuvette to obtain the desired micellar system by the addition of more nonpolar solvent ([AOT] = 0.1 M). Then, the necessary volume of AP stock solution ($5x10^{-5}$ M) was added to obtain a final enzyme concentration equal to $1x10^{-7}$ M. After thermostat for 10 min, a certain amount of buffer solution and 1-naphthyl phosphate stock solution (in buffer solution) were added to reach both the W_0 and [1-naphthyl phosphate] desired, with which the reaction begins. The final volume was 2 mL.

1.2.3 Kinetic Procedure

The enzymatic hydrolysis reaction of 1-naphthyl phosphate was followed by determining the UV-vis absorbance of the 1-naphthol or 1-naphtholate product, depending on the reaction media, at 280 nm and 323 nm, respectively, using a UV-vis spectrophotometer (HP / Agilent 8453), with a cell thermostatted at 35 ± 0.2 °C.

As the substrate 1-naphthyl phosphate and the enzyme AP are both hydrophilic compounds, they are insoluble in organic solvents. Consequently in RMs, they are located in the micellar interior and are not partitioned with the external nonpolar solvent.[2–6] Thus, the reaction of 1-naphthyl phosphate catalyzed by AP can be treated according to the well-known Michaelis-Menten theory[7,8], whose mechanism is presented in the following equation S1:

$$E + S \underset{k_{-1}}{\overset{k_1}{\rightleftarrows}} E\text{-}S \overset{k_{cat}}{\rightarrow} E + P$$

(S1)
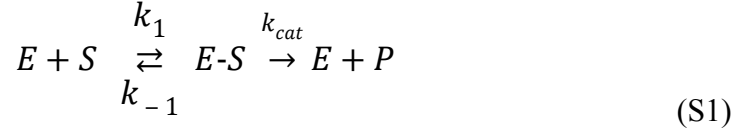
Where E, S, E-S, and P represent the enzyme, substrate, enzyme-substrate complex, and product, respectively.

Applying the steady-state approximation to E-S, the rate law given in equation S2 is obtained:

$$\frac{v_0}{[E]} = \frac{k_{cat}[S]}{K_M + [S]}$$

(S2)

where v_0 is the initial reaction rate, [E] is the analytical enzyme concentration, [S] is the analytical concentration of the substrate, k_{cat} is the catalytic rate constant, and K_M is the Michaelis constant defined as:

$$K_M = (k_{-1} + k_{cat}) / k_1$$

(S3)

The ratio k_{cat}/K_M is known as catalytic efficiency. The absorbance was recorded as a function of time, and the initial velocity was obtained from the slope of the concentration of the product versus time profiles (considering the initial stage of the reaction). Thus, the v_0 values were plotted as a function of the substrate concentration; then, a fit was made according to equation S2 to obtain k_{cat} and K_M values. For example, from the absorption spectra at different times (Figure 1), plots such as Figure S1 with the absorption values at 336 nm as a function of time can be made. Then, dividing these absorption values by the molar

absorptivity coefficient of 1-naphtolate determined experimentally ($\varepsilon = 4136$ M^{-1}cm^{-1}, see Table S1), the concentration of 1-naphtolate is obtained and plotted against the time (Figure S2). Then, the initial velocity (v_0) was determined from the slope of the linear zone (initial time values) of the graph of Figure S2 using equation S4.

$$v_0 = \frac{1}{\varepsilon_{exp}}\left(\frac{dA_{336}}{dt}\right) \qquad \text{(S4)}$$

For the AOT RMs experiments, a similar procedure was performed[9–11] but, in these cases, the molar absorptivity coefficient of 1-naphthol (at $\lambda = 323$ nm) determined in every RMs was employed (See Table S1).

The pooled standard deviation of the kinetic data, by using different samples, was less than 5%.

Table S1. Molar absorptivity values (ε) for the 1-naphthyl phosphate in the different systems. $W_0 = 10$.

Media	ε^{323} $(M^{-1}cm^{-1})$
Water	4136 ± 207[a]
n-heptane/AOT/water	2175 ± 108
benzene/AOT/water	1925 ± 96
isopropyl myristate/AOT/water	2290 ± 114
methyl laurate/AOT/ water	2161 ± 103

[a] ε for 1-Naphtholate (at $\lambda = 336$ nm).
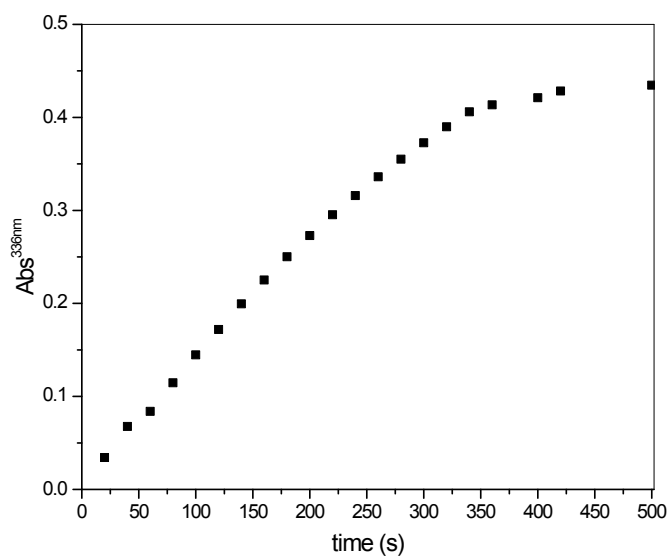
Figure S1. Changes in absorbance value at 336 nm as a function of time for the hydrolysis of 1-naphthyl phosphate catalyzed by AP in $Na_2CO_3/NaHCO_3$ buffer solution, at 35°C. [1-naphthyl phosphate] = $2x10^{-4}$ M. [AP] = $1x10^{-7}$ M. [buffer] = 0.01 M, pH = 10.
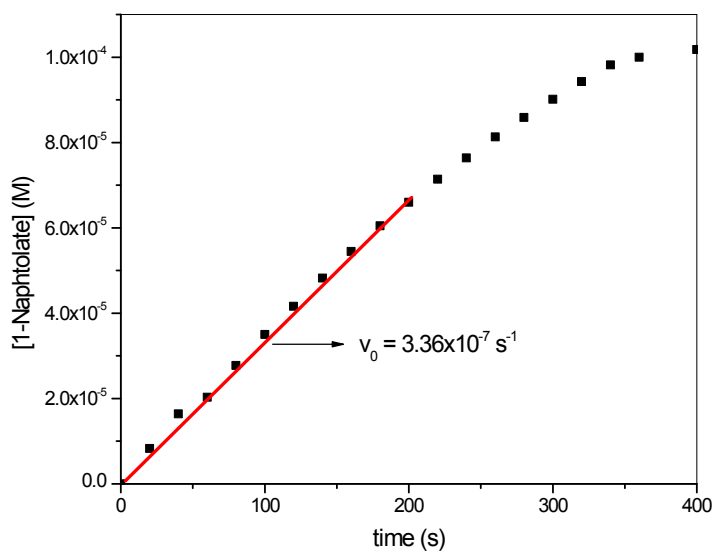
Figure S2. Variation of the concentration of the product 1-naphtholate in $Na_2CO_3/NaHCO_3$ buffer solution at different reaction times. T = 35°C. [1-naphthyl phosphate] = $2x10^{-4}$ M. [AP] = $1x10^{-7}$ M. [buffer] = 0.01 M, pH = 10. The solid line represents the fit according to equation S4.
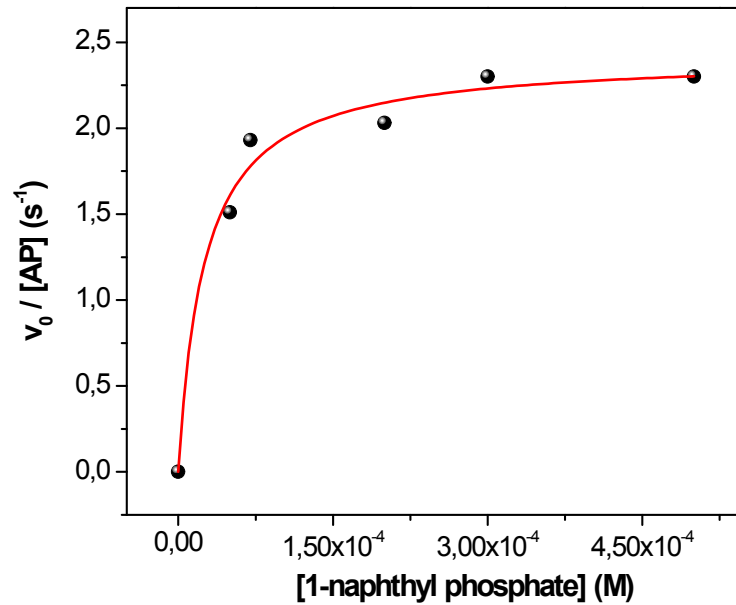
Figure S3. Effect of 1-naphthyl phosphate concentration on the initial rate (v_0) of 1-naphthyl phosphate hydrolysis catalyzed by AP in methyl laurate/AOT/water, at 35°C. $W_0 = 10$. [AP] $= 1 \times 10^{-7}$ M. [Na_2CO_3/$NaHCO_3$] $= 0.01$ M, pH $= 10$. The solid line represents the fit according to equation 1.
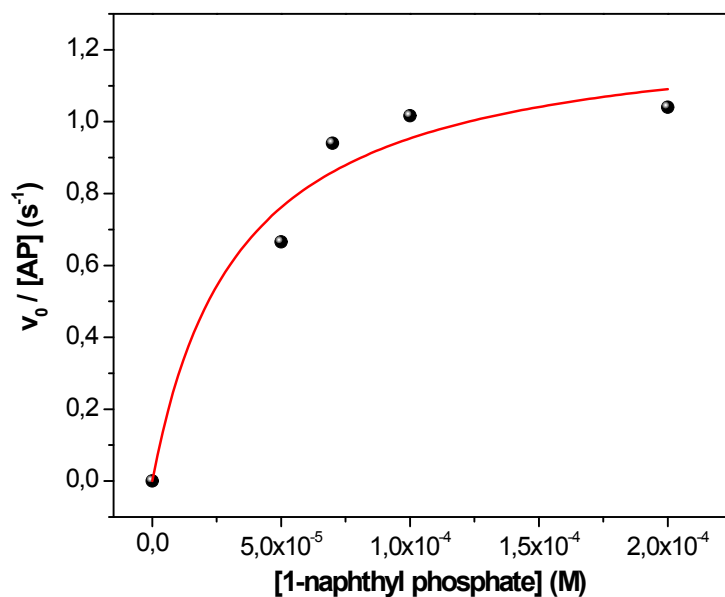
Figure S4. Effect of 1-naphthyl phosphate concentration on the initial rate (v_0) of 1-naphthyl phosphate hydrolysis catalyzed by AP in benzene/AOT/water, at 35°C. W_0 = 10. [AP] = $1x10^{-7}$ M. [$Na_2CO_3/NaHCO_3$] = 0.01 M, pH = 10. The solid line represents the fit according to equation 1.
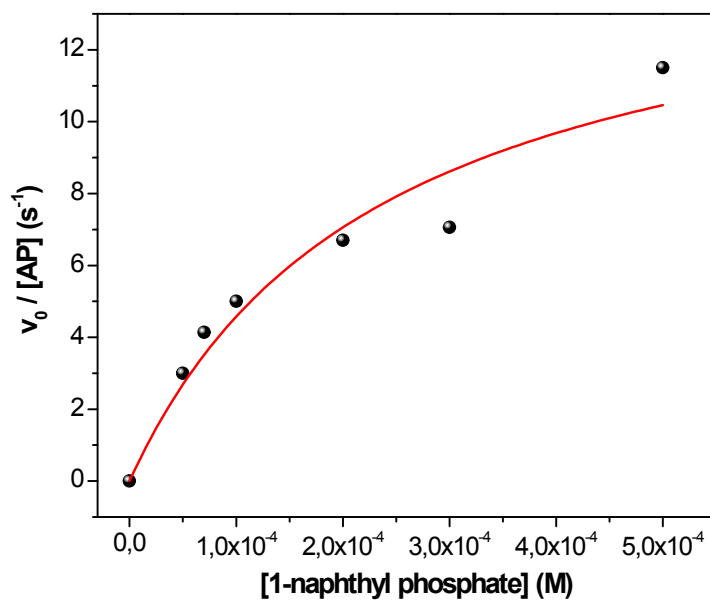
Figure S5. Effect of 1-naphthyl phosphate concentration on the initial rate (v_0) of 1-naphthyl phosphate hydrolysis catalyzed by AP in *n*-heptane/AOT/water, at 35°C. $W_0 = 10$. [AP] = 1×10^{-7} M. [$Na_2CO_3/NaHCO_3$] = 0.01 M, pH = 10. The solid line represents the fit according to equation 1.

References

1   N. M. Correa, M. A. Biasutti and J. J. Silber, *J. Colloid Interface Sci.*, 1995, **172**, 71–76.

2   S. Gupta, L. Mukhopadhyay and S. P. Moulik, *Colloids Surfaces B Biointerfaces*, 1994, **3**, 191–201.

3   H.-C. Hung, T.-M. Huang and G.-G. Chang, *J. Chem. Soc. Perkin Trans. 2*, 1997, 2757–2760.

4   J. Fenoll, *Talanta*, 2002, **56**, 1021–1026.

5   R. Bansal-Mutalik and V. G. Gaikar, *Biotechnol. Prog.*, 2003, **19**, 1713–1720.

6   R. Bansal-Mutalik and V. G. Gaikar, *Biotechnol. Prog.*, 2004, **20**, 1121–1127.

7   R. M. D. VERHAERT, R. HILHORST, M. VERMUE, T. J. SCHAAFSMA and C. VEEGER, *Eur. J. Biochem.*, 1990, **187**, 59–72.

8   E. A. Lissi and E. B. Abuin, *Langmuir*, 2000, **16**, 10084–10086.

9   E. I. Gomez Rodríguez, R. D. Falcone, P. R. Beassoni, F. Moyano and N. M. Correa, *ChemistrySelect*, 2019, **4**, 7204–7210.

10   R. D. Falcone, M. A. Biasutti, N. M. Correa, J. J. Silber, E. Lissi and E. Abuin, *Langmuir*, 2004, **20**, 5732–5737.

11   F. Moyano, E. Setien, J. J. Silber and N. M. Correa, *Langmuir*, 2013, **29**, 8245–8254.